Novel Potent BRAF Inhibitors: Toward 1 nM Compounds through Optimization of the Central Phenyl Ring

Delphine Ménard,[†] Ion Niculescu-Duvaz,[†] Harmen P. Dijkstra,[†] Dan Niculescu-Duvaz,[†] Bart M. J. M. Suijkerbuijk,[†] Alfonso Zambon,[†] Arnaud Nourry,[†] Esteban Roman,[†] Lawrence Davies,[†] Helen A. Manne,[†] Frank Friedlos,[†] Ruth Kirk,[‡] Steven Whittaker,[‡] Adrian Gill,[§] Richard D. Taylor,[§] Richard Marais,[‡] and Caroline J. Springer*[,†]

The Institute of Cancer Research, UK Centre for Cancer Therapeutics, 15 Cotswold Road, Sutton, Surrey SM2 5NG, United Kingdom, The Institute of Cancer Research, UK Centre for Cell and Molecular Biology, 237 Fulham Road, London SW3 6JB, United Kingdom, and Astex Therapeutics Ltd., 436 Cambridge Science Park, Cambridge CB4 0QA, United Kingdom

Received February 25, 2009

BRAF, a serine/threonine specific protein kinase that is part of the MAPK pathway and acts as a downstream effector of RAS, is a potential therapeutic target in melanoma. We have developed a series of small-molecule BRAF inhibitors based on a 1*H*-imidazo[4,5-*b*]pyridine-2(3*H*)-one scaffold (ring A) as the hinge binding moiety and a number of substituted phenyl rings C that interact with the allosteric binding site. The introduction of various groups on the central phenyl ring B combined with appropriate A- and C-ring modifications afford very potent compounds that inhibit ^{V600E}BRAF kinase activity in vitro and oncogenic BRAF signaling in melanoma cells. Substitution on the central phenyl ring of a 3-fluoro, a naphthyl, or a 3-thiomethyl group improves activity to yield compounds with an IC_{50} of 1 nM for purified ^{V600E}BRAF and nanomolar activity in cells.

Introduction

The RAF family of protein kinases are serine/threonine specific protein kinases that are key players in the mitogen activated protein (MAP) kinase pathway. These proteins act immediately downstream of Ras to conduct extracellular signals from the cell membrane to the nucleus via a cascade of phosphorylation events, thereby regulating cell growth, proliferation, and differentiation in response to growth factors, cytokines, and hormones.[1] The v-Raf murine sarcoma viral oncogene homologue B1 (BRAF[a])[2] is frequently mutated to generate active forms in human cancer, with the most frequent mutation occurring at position 600 as a glutamic acid for valine substitution (V600E; 90%).[3] ^{V600E}BRAF is ∼500-fold more active than the wild-type protein,[4] and in cutaneous malignant melanoma, these mutations occur with a frequency of 50−70%. BRAF mutations are also present in a range of other human cancers, particularly thyroid (30%), colorectal (10%), and ovarian (35%) cancers.[3] Importantly, inhibition of BRAF signaling blocks cancer cell proliferation and induces apoptosis, validating ^{V600E}BRAF as a therapeutic target[5] and offering opportunities for anticancer drug development.

The interest in developing new drugs targeting the MAP kinase pathway has increased considerably, and inhibitors are currently being tested in preclinical and clinical trials.[6] Despite the fact that early detection and improved surgical techniques has led to increased survival of melanoma patients, the prognosis of patients with disseminated disease remains disappointing. Several small molecule inhibitors acting at different levels in the MAPK pathway have been described, such as PD0325901[7] and AZD6244,[8] which target MEK, the downstream target of BRAF, and PLX4032[9] and RAF265,[10] which target ^{V600E}BRAF. Some of these drugs have progressed to clinical evaluation.[11,12]

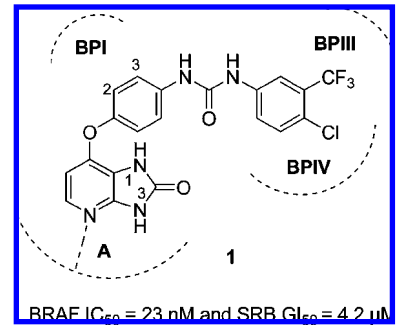

Figure 1. Structure of the pyridoimidazolone BRAF inhibitor **1** and its proposed binding mode with BRAF.

We have previously described the development of new ^{V600E}BRAF inhibitors based on a disubstituted pyrazine scaffold,[13,14] and more recently we reported on a novel series of BRAF inhibitors, exemplified by 1*H*-imidazo[4,5-*b*]pyridine-2(3*H*)-one **1** (see Figure 1), which are based on an innovative hinge-binding fragment.[15] The proposed binding mode is shown in Figure 1 and is based on an analogy to the crystal structure of BRAF with sorafenib, which was previously resolved by us.[4]

We demonstrated good activity with these inhibitors against purified ^{V600E}BRAF, but these compounds were only weakly active at inhibiting cell proliferation, with GI_{50} values of over 1 μM.[15] The compounds we previously reported contain an unsubstituted phenyl ring B. To improve the potency of these compounds on both the isolated enzyme and on cell lines driven by oncogenic BRAF, we anticipated that appropriate functionalization of the phenyl ring B would lead to the desired gain in potency in cells. Assuming a binding mode similar to that of sorafenib, an examination of this cocrystal structure revealed a space in the lipophilic pocket adjacent to the adenine binding site formed in the DFG-out conformation (BP-I pocket),[16] which would be available to accommodate these ring B substitutions. These modifications might simultaneously provide a potential means of increasing the selectivity of inhibitors toward mutant BRAF (see Table 1).

* To whom correspondence should be addressed. Phone: +44 20 8722 4214. Fax: +44 20 8722 4046. E-mail: caroline.springer@icr.ac.uk.
[†] The Institute of Cancer Research, UK Centre for Cancer Therapeutics.
[‡] The Institute of Cancer Research, UK Centre for Cell and Molecular Biology.
[§] Astex Therapeutics Ltd.

[a] Abbreviations: BRAF, V-RAF murine sarcoma viral oncogene homologue B1; MAPK, mitogen-activated protein kinase; MEK, MAPK/ERK kinase; ERK, extracellular regulated kinase; Boc, *tert*-butoxycarbonyl; TFA, trifluoroacetic acid; THF, tetrahydrofuran; DCM, dichloromethane; DMF, dimethylformamide; DMSO, dimethylsulfoxide; atm, atmosphere.

10.1021/jm900242c CCC: $40.75
Published on Web 05/27/2009

Table 1. Effect of Modification of the Central Phenyl Ring of Inhibitor **1**

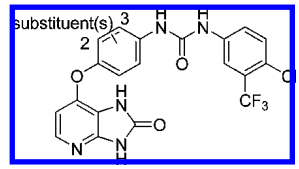

Compound number	Central phenyl ring	^{V600E}BRAF IC_{50} (μM)	pERK IC_{50} (μM)	SRB GI_{50} (μM)
1	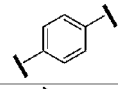	0.023	2.39	4.2
21a	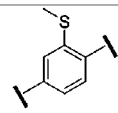	0.001	0.61	0.47
21b	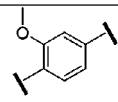	0.025	5.5	6.2
21c	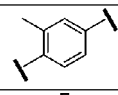	0.023	59	1.79
21d	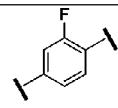	0.008	2.17	1.53
21e	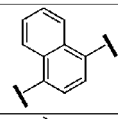	0.030	0.559	0.47
21f	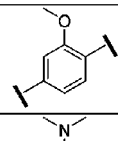	0.106	>100	ND
21g	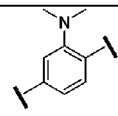	10	20.7	5.34
21h	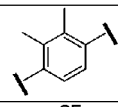	0.056	3.9	2
21i	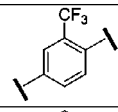	0.022	3.58	0.93
21j	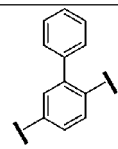	6.5	>100	5.1
21k	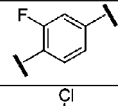	0.047	34	ND
21l	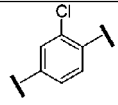	0.021	1.33	2
21m	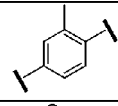	0.037	4.72	5.9
26	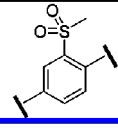	0.090	11.0	11.9

Scheme 1. Two Synthetic Routes Employed to Generate Novel BRAF Inhibitors

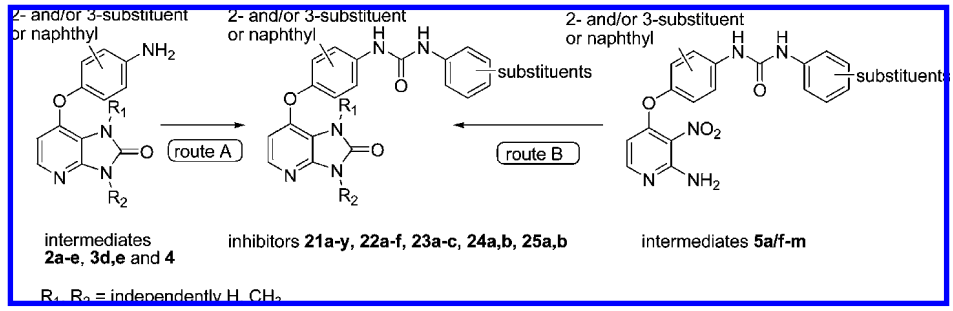

In this paper, we show that several ring B modifications improve the activity of this class of inhibitor on both purified ^{V600E}BRAF in vitro and on oncogenic BRAF signaling in cells.

Chemistry

The target compounds **21a**−**y**, **22a**−**f**, **23a**−**c**, **24a**,**b**, and **25a**,**b** were obtained via the two routes described in Scheme 1. In route A, the A−B system is first fully synthesized, whereafter ring C is attached. Route B relies on the introduction of ring C before the formation of the 1*H*-imidazo[4,5-*b*]pyridine-2(3*H*)-one A ring. Route A has the key advantage that it generates final compounds with different C rings readily and within a few steps from advanced amino intermediates such as **2a**−**e**, **3d**,**e**, and **4** summarized in Figure 2. Route B, developed due to the difficulties encountered in protecting the amino group on the phenyl ring B of some intermediates **9**, generates final compounds in only three steps from intermediates **5a**/**f**−**m**.

Whichever route is used, the first step is a coupling reaction between 2-amino-4-chloro-3-nitropyridine and an appropriately functionalized 4-aminophenol or 4-amino-1-naphthol. Only intermediate **4** required 4-chloro-3-nitro-2-*N*-methylaminopyridine intermediate **17**, whose synthesis has already been described.[15] Substituted nitrophenols **6b**−**d**/**h**,**i** were commercially available; intermediates **6a**, **6f**,**g** and **7j** were synthesized. Substitution of the fluorine atom in the 3-fluoro-4-nitrophenol afforded the corresponding 3-thiomethyl− (**6a**), 3-methoxy− (**6f**),[17] and 3-dimethylamino-4-nitrophenol (**6g**)[18] intermediates (Scheme 2). 3-Phenyl-4-aminophenol **7j** was synthesized in three steps by Avenova's method[19] via a

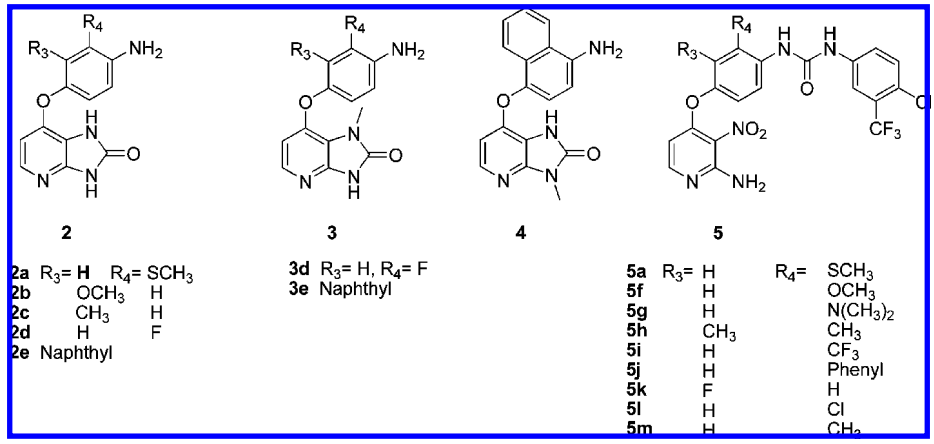

Figure 2. Key intermediates for the synthesis of BRAF inhibitors.

Scheme 2. Preparation of Substituted Aminophenol Ring B Starting from the Commercially Available 3-Fluoro-4-nitrophenol[a]

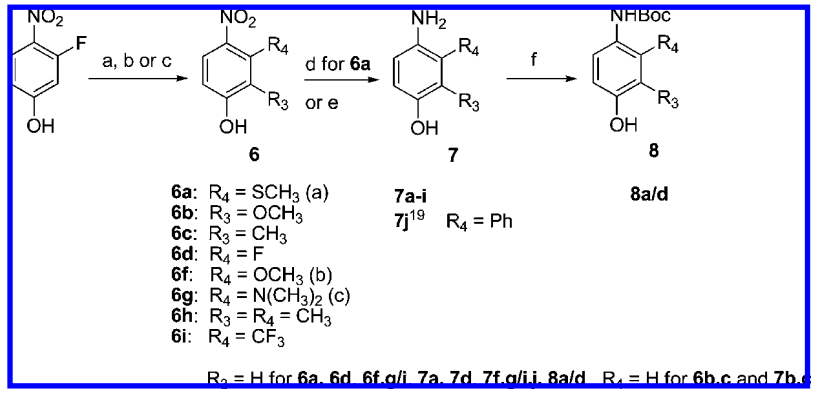

[a] Reagents and conditions: (a) NaSMe, K_2CO_3, DMF; (b) NaOMe, MeOH, reflux; (c) $(CH_3)_2NH\cdot HCl$, K_2CO_3, DMSO/H_2O, 100 °C; (d) Fe, NH_4Cl, EtOH/H_2O, reflux; (e) Pd/C, H_2, RT, (f) Boc_2O, $InCl_3$, 35 °C.

Scheme 3. Synthesis of Key Intermediates **2a**−**e**[a]

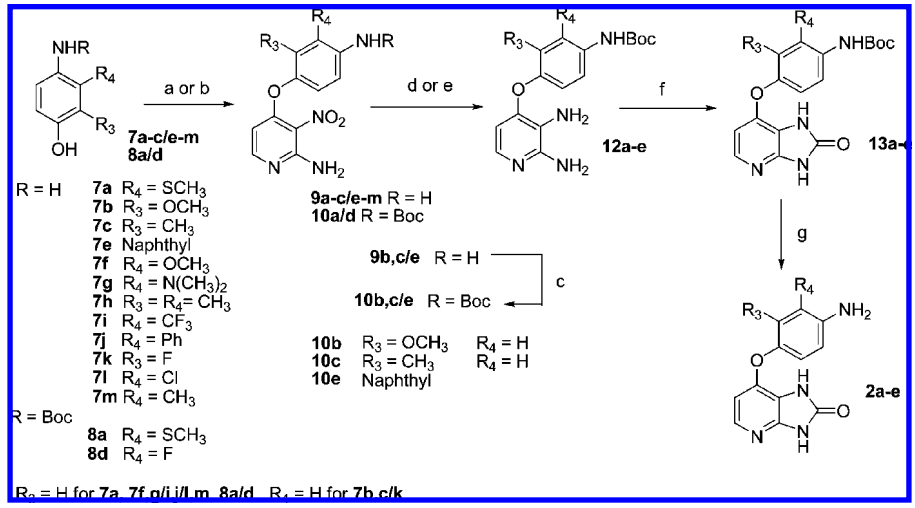

[a] Reagents and conditions: (a) 2-amino-4-chloro-3-nitropyridine, tBuOK, DMF, 70 °C; (b) 2-amino-4-chloro-3-nitropyridine, NaH, DMSO, 100 °C; (c) Boc_2O, THF; (d) Pd/C, H_2, RT; (e) Fe, NH_4Cl, $EtOH/H_2O$ for **10a**; (f) $(Cl_3CO)_2CO$, pyridine, THF; (g) TFA.

Scheme 4. Synthesis of Key Intermediates **3d**−**e**[a]

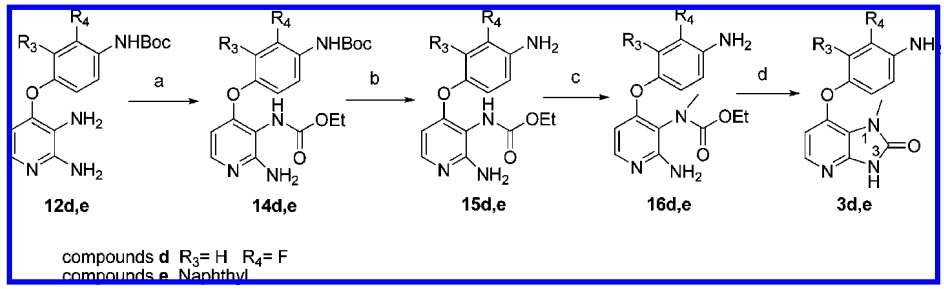

[a] Reagents and conditions: (a) EtOCOCl, pyridine, THF; (b) TFA; (c) MeI, NaH, THF; (d) EtONa, EtOH, microwave condition.

Scheme 5. Synthesis of Key Intermediate **4**[a]

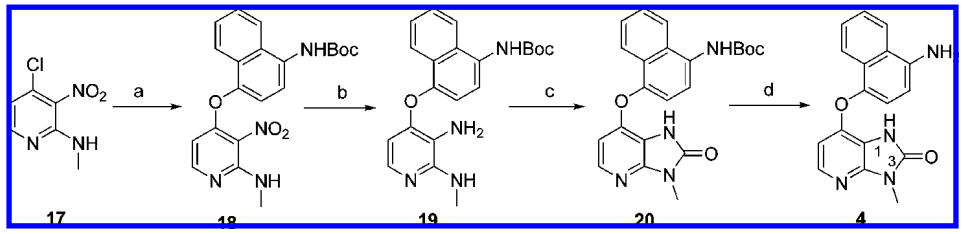

[a] Reagents and conditions: (a) 4-(*N*-Boc-amino)naphthol, tBuOK, DMF, 70 °C; (b) H_2, Pd/C, EtOH; (c) triphosgene, pyridine, THF; (d) TFA.

Diels−Alder cycloaddition of (*Z*)-4-benzylidene-2-phenyl-2-oxazolin-5-one with Danishefsky's diene.

Substituted *p*-nitrophenol compounds **6b**−**d**/**f**−**i** were reduced by catalytic hydrogenation over Pd/C to provide *p*-aminophenols **7b**−**d**/**f**−**i**. Reduction of **6a** required the use of iron as the thiomethyl group poisoned Pd/C and Raney nickel catalysts. Ammonium chloride[20] was preferred to acetic acid[21] as a proton source because the latter reaction gave 20% of the undesired corresponding acetamide. Subsequent protection of the amino group as required for route A was readily achieved using Boc_2O and catalytic $InCl_3$ (1 mol %)[22] at 35 °C to generate **8a** and **8d**.

Coupling of the functionalized phenols with 2-amino-4-chloro-3-nitropyridine is presented in Scheme 3. NaH in DMSO is preferred to tBuOK in dry DMF, as 4-(2-amino-3-nitropyridin-4-ylamino) substituted phenols were formed as side products (10 to 100%) in the latter case. The use of NaH provided only the expected ether-linked compounds **9a**−**c**/**e**−**m** in high yields and purities. Compounds **10a**/**d** were synthesized in a similar way.

Protection of the amino group of intermediates **9a**−**c**/**e** was carried out using Boc_2O in THF at room temperature. However, the presence of bulky groups at the 3-position of the ring B (see Figure 1 for numbering) and the electronic effects of the substituents led to slow reactions for compounds **9l** and **9m** and a total lack of reactivity for compound **9a**. The use of $InCl_3$ (1 mol %) considerably improved the yield to 90% after 4 h at 35 °C for **9a**. From this stage on, key intermediates **2a**−**e**, **3d**,**e**, and **4** were obtained by following a similar synthetic route described previously by Niculescu-Duvaz et al.[15] (Schemes 3, 4, and 5). Reduction of the 3-nitropyridine group of protected intermediates **10a**−**e** gave intermediates **12a**−**e**. Cyclisation of the diamino pyridyl derivative with triphosgene, followed by

Table 2. Combinations of Various Substituted Phenyl Rings C with the Optimal Rings B

Compound number	Ring C	Ring B[a]	^{V600E}BRAF IC_{50} (μM)	pERK IC_{50} (μM)	SRB GI_{50} (μM)
21a	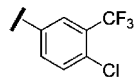	SMe	0.001	0.61	0.47
21d		F	0.008	2.17	1.53
21e		Naphthyl	0.030	0.559	0.47
21n	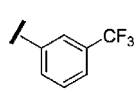	SMe	0.001	1.3	1.06
21p		OMe	0.016	29.4	>100
21q		F	0.012	3.45	1.61
21t		Naphthyl	0.006	1.91	0.32
21o	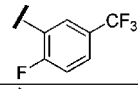	SMe	0.012	3.06	2.6
21r		F	0.007	1.29	1.15
21u		Naphthyl	0.037	0.214	0.29
21s	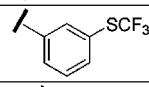	F	0.007	4.15	1.19
21v	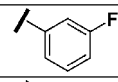	Naphthyl	0.22	>100	5.5
21w	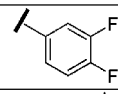	Naphthyl	0.079	19.3	3.9
21x	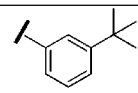	Naphthyl	0.014	0.346	0.291
21y	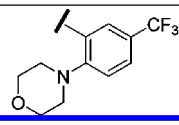	Naphthyl	0.638	1.57	0.89

[a] All substitutions occurred in position 3 of the phenyl ring B with the exception of inhibitor **21p** substituted in position 2.

deprotection of the ring B amino group with trifluoroacetic acid, afforded intermediates **2a**−**e** (Scheme 3).

Intermediates **3d**,**e** were obtained in four steps from compounds **12d** and **12e**.[15] First the diamino-intermediates **12d**,**e** were acylated in position N1 with ethyl chloroformate, after which the Boc amino group protection was removed with TFA to give intermediates **15d**,**e**. Selective methylation of the carbamate nitrogen using MeI and NaH, followed by an intramolecular cyclization using microwave irradiation produced imidazolones **3d** and **3e**, which are methylated at position N1 (Scheme 4).

The synthesis of 3-*N*-methylated intermediate **4** is similar to the synthesis described previously for the common intermediates **2a**−**e**, the only difference being the first step coupling of 4-chloro-3-nitro-2-*N*-methylaminopyridine **17**[15] and 4-(*N*-Boc-aminonaphthol) (Scheme 5).

The final compounds **21b**−**e**/**n**−**y** were obtained after coupling key intermediates **2a**−**e**, **3e**, and **4** with several substituted aryl isocyanates in dry THF at room temperature (Scheme 6). Compounds **24a**,**b** with a methylene amide linker and compounds **25a**,**b** with an amide linker resulting from condensation of the corresponding substituted benzoyl chloride or phenylacetyl chloride with intermediates **2e** and **3e** in dioxane in the presence of triethylamine under an inert atmosphere at 80 °C for 20 h (Scheme 7).

As the protection of some 4-(4-substituted aminophenoxy)-3-nitropyridin-2-amines failed when using the conventional procedure, route B was explored and the formation of ring A was performed as the last step (Scheme 8). Thus, the rings C were introduced by coupling intermediates **9a**/**f**−**m** with 4-chloro-3-trifluoromethylphenyl isocyanate in DCM at room temperature to form **5a**/**f**−**m**. The subsequent nitro group reduction was performed using conditions previously described for the starting substituted nitrophenol, i.e., Pd/C catalyst, H_2, or iron with NH_4Cl (**9a**) to provide the corresponding 2,3-diaminopyridin-4-yloxy intermediate **11a**/**f**−**m**. Finally, formation of the imidazolone ring was performed using triphosgene with pyridine in THF at room temperature to afford compounds **21a**/**f**−**m**.

Oxidation of the thiomethyl group of **21a** using oxone in water at 0 °C yielded the corresponding sulfoxide compound **26**.

Results and Discussion

Our aim was to improve the potency and the cellular activity of **1** by exploring the influence of modifications to ring B. To compare the biological data from this modified series with the unsubstituted **1**, we kept constant the 1*H*-imidazo[4,5-*b*]pyridine-2(3*H*)-one ring A, which binds to the hinge region, the urea linker B−C and the 3-trifluoromethylphenyl substituted ring C, which interact with the DFG-pocket (BP-III and BP-IV).[16]

The biological activities of all compounds were tested in vitro using three assays: (a) the determination of the IC_{50} against the isolated ^{V600E}BRAF enzyme (IC_{50}, BRAF), (b) the determination of the growth inhibition by SRB (GI_{50}, SRB) of WM266.4 human melanoma cells that are driven by mutant BRAF, (c) compounds were also tested for cellular inhibition of the target pathway (IC_{50} of ERK phosphorylation in WM266.4 melanoma cells-IC_{50}, pERK)[23] (see Table 1).

Modifications on Ring B. All the modifications of ring B yield compounds that inhibit oncogenic BRAF except substitu-

Table 3. Effect of Modification of Ring A and Ring C in the Naphthyl Series

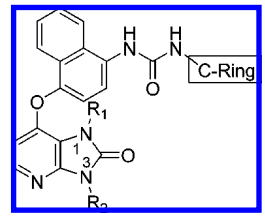

Compound number	Ring C	R_1, R_2 (Ring A)	^{V600E}BRAF IC_{50} (μM)	pERK IC_{50} (μM)	SRB GI_{50} (μM)
21e	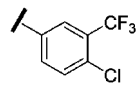	H, H	0.030	0.559	0.47
22b		CH_3, H	0.023	0.77	1.04
23a		H, CH_3	0.156	3.14	2.3
21u	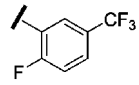	H, H	0.037	0.214	0.29
22c		CH_3, H	0.017	0.81	0.49
23b		H, CH_3	0.167	2.0	0.73
21x	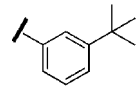	H, H	0.014	0.346	0.291
22d		CH_3, H	0.037	1.06	1.13
23c		H, CH_3	0.43	46	>100
21t	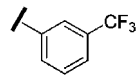	H, H	0.006	1.91	0.32
22e		CH_3, H	0.010	0.60	0.81
22f	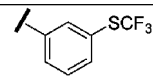	CH_3, H	0.024	1.46	1.2

tion in the 3-position with a phenyl (**21j**) or a dimethylamino group (**21g**) that lead to inactive compounds (see Table 1). The replacement of the phenyl with a naphthyl ring is beneficial.

The introduction of a methyl or a fluoro group at position 3 (**21m**, **21d**) confers greater potency to the compounds than the same substitution at position 2 (**21c**, **21k**). Despite good activity against the ^{V600E}BRAF enzyme (0.023 and 0.047 μM compared to 0.037 and 0.008 μM, respectively) a drop of 12- to 16-fold in potency on pERK is observed. Unexpectedly, the reverse is seen with a methoxy group (the 2-methoxy compound **21b** is more potent on IC_{50} BRAF and IC_{50} pERK than its 3-methoxy analogue **21f**), although no improvement is achieved with respect to the parent compound **1** with an unsubstituted central phenyl ring.

In general, hydrophobic groups such as halogens, especially fluorine, are beneficial for potency on ^{V600E}BRAF (BRAF IC_{50} = 0.023 μM for a chlorine **21l** and 0.008 μM for a fluorine **21d**). However, inhibition of pERK activity in cells (IC_{50} ppERK) and inhibition of proliferation (SRB GI_{50}) remain above 1 μM. The presence of a trifluoromethyl group (**21i**) enhances the activity on SRB by 4.5-fold to afford a submicromolar compound at 0.93 μM.

Two ring B modifications show considerable overall improvements compared to **1**. A 3-thiomethyl substituent on phenyl ring B improves the BRAF potency to an IC_{50} of 1 nM (**21a**) and shows good activity on cells with pERK IC_{50} at 0.61 μM and SRB GI_{50} at 0.47 μM. The use of the naphthyl system as ring B (**21e**), despite having a modest negative effect on BRAF potency (BRAF IC_{50} of 30 nM), sharply increases the cellular activity of these compounds (pERK IC_{50} of 0.56 μM and SRB GI_{50} of 0.47 μM).

Isosteric replacements of the 3-thiomethyl substituent with other heteroatom groups did not lead to equipotent or more potent compounds. A methoxy group (**21f**) decreased drastically the cell activity to greater than 100 μM, even though it showed a relatively good BRAF activity at 0.106 μM. A dimethylamino substituent (**21g**) is not tolerated. The oxidation of the thiomethyl group of **21a** to a methylsulfonyl group (**26**) also reduces both the cellular activity and the activity against BRAF. Similarly, replacing the naphthyl group by a 2,3-dimethylphenyl ring (**21h**) is detrimental.

These results clearly show that the modification of the phenyl middle ring can greatly enhance the activity of the compounds. The substitution of the phenyl B ring in position 3 leads to more potent inhibitors than in position 2. Hydrophobic groups enhance the activity on cells providing submicromolar compounds in pERK and SRB assays; the most promising groups are 3-thiomethyl, 3-fluorine, or replacement of the phenyl ring with naphthyl.

Variation of Ring C. We investigated the effect of ring C when combined with the most beneficially substituted middle ring B, following our improvements to the potency of **1** against

Table 4. Compounds with Amide or Methylene Amide Linker B−C

Compound number	Compound	^{V600E}BRAF IC_{50} (μM)	PERK IC_{50} (μM)	SRB GI_{50} (μM)
24a	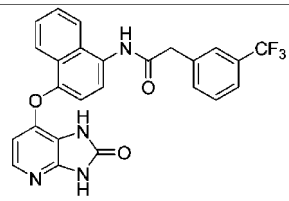	>10	>100	ND
24b	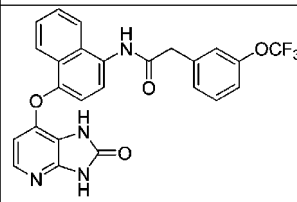	>10	>100	3.1
25a	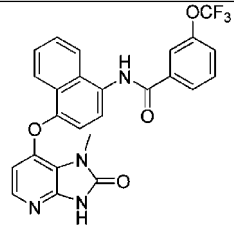	5.2	31	12
25b	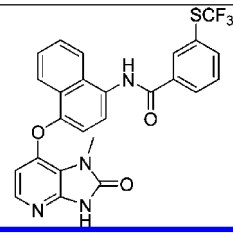	4.6	18.4	7.6

^{V600E}BRAF and also on cells by modification of the phenyl ring B. We selected C rings that had been identified as active,[15] and we combined them with the 3-fluoro, 3-thiomethylphenyl, and naphthyl rings B (see Table 2).

Replacement of the chlorine atom of ring C for a hydrogen atom does not affect the activity against isolated ^{V600E}BRAF for inhibitors with a 3-fluoro− (**21q**) or a 3-thiomethyl (**21n**) substituted phenyl ring B, but the potency on cells decreases by approximately 1.5-fold. In contrast, the naphthyl compound **21t** shows an enhancement on both BRAF IC_{50} and SRB GI_{50}, but the inhibition of pERK decreases by more than 3-fold.

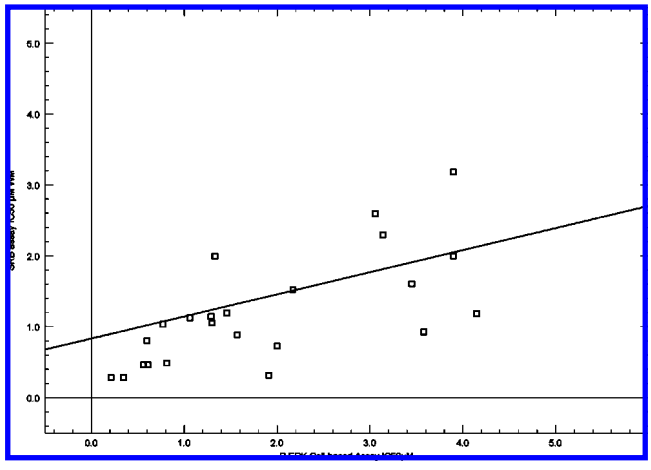

Figure 3. Graph showing the linear relationship between pERK IC_{50} and SRB GI_{50}.

Replacement of the trifluoromethyl group with the more lipophilic trifluoromethylthio group (**21s**) has no effect on the potency on the isolated enzyme or on cellular assays. However, replacing the trifluoromethyl group by a *tert*-butyl group (**21x**) (naphthyl substituted ring B) enhances the potency on all three assays by almost 2-fold.

Compounds with a 3-trifluoromethyl-6-fluoro phenyl ring C are less active in cellular potency assays for the 3-fluoro **21r** and 3-thiomethyl **21o** compounds despite having a good activity against ^{V600E}BRAF. In contrast, the combination of this ring with naphthyl ring B (**21u**) increases the potency on cells. Increasing the bulk on position 2 by introducing a morpholino group leads to a decrease of the activity in all three assays.

Among the different rings C investigated, the 3-trifluoromethyl-6-fluorophenyl or a 3-*tert*-butylphenyl group when combined with a naphthyl middle ring achieve the greatest potency against ^{V600E}BRAF, cellular ERK phosphorylation, and cell growth inhibition.

***N*-Methylation of Ring A.** We have shown previously that methylation of the pyridoimidazolone improves the pharmacokinetic (PK) profile of our compounds by eliminating an H-bond donor while preserving good ^{V600E}BRAF and cellular activities.[15] We therefore combined the naphthyl ring B with the methylated pyridoimidazolone ring A and with different rings C.

Of the compounds containing 4-chloro-3-trifluoromethylphenyl **22b**, a 3-trifluoro-6-fluoro-methylphenyl **22c** or a 3-*tert*-

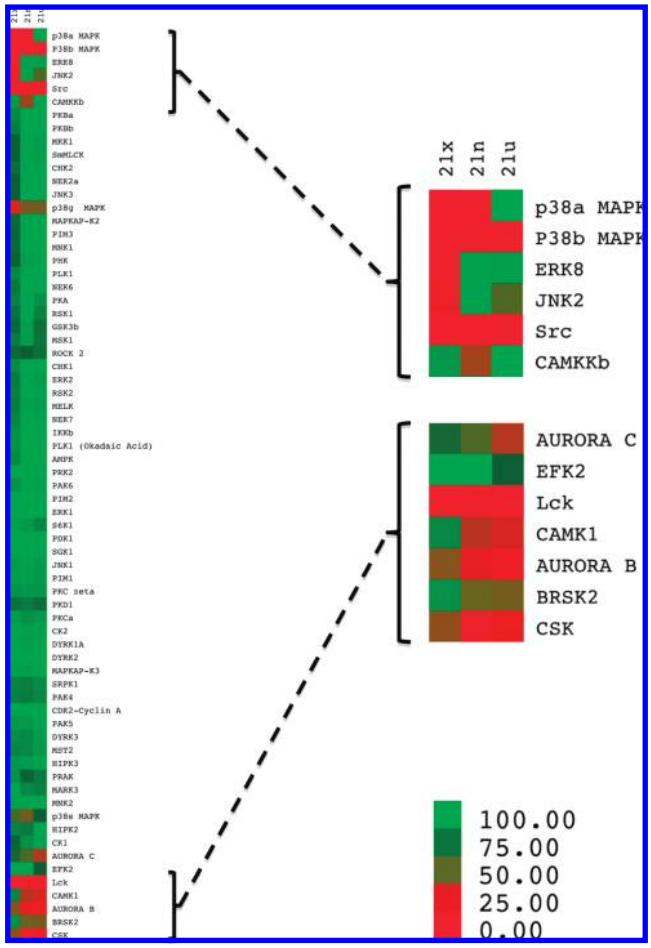

Figure 4. Kinase selectivity of compounds **21n**, **21u**, and **21x**. Compounds were tested against a panel of 69 kinases at the MRC National Centre for Protein Kinase Profiling. The color bar represents percent activity relative to the control.

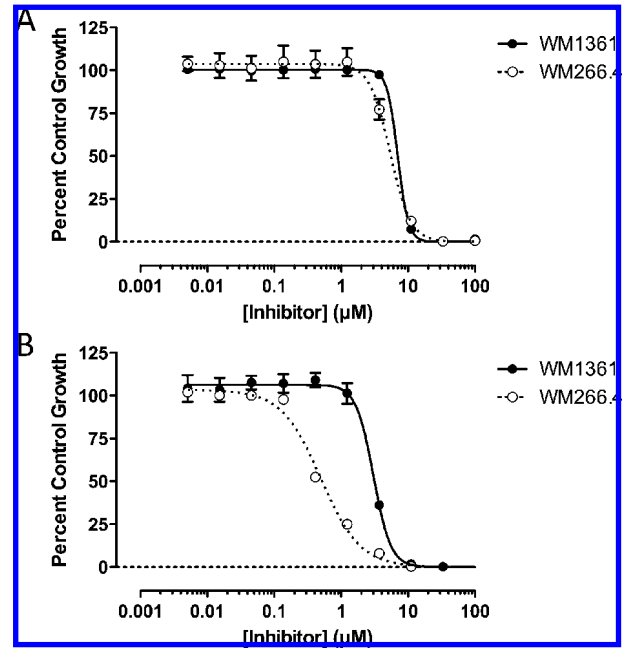

Figure 5. Selective inhibition of a mutant BRAF-driven human melanoma cell line displayed with **22c**. Growth inhibition of WM266.4 (BRAF mutant) and WM1361 (NRAS mutant) melanoma cell lines following a 5 day exposure to sorafenib (A) or **22c** (B) and analysis by SRB assay.

butylphenyl **22d** ring C, the methylation on the N1 position is tolerated with an effectively unchanged activity on ^{V600E}BRAF, despite some detrimental effect on cellular activity compared to the nonmethylated counterparts **21e**, **21u**, and **21x** (see Table 3). The 3-trifluoromethylphenyl ring C (**22e**) combined with the *N*1-methylated ring A is active with only a slight loss of potency in the SRB assay. Again, a 3-trifluorothiomethylphenyl ring C (**22f**) has no positive effect on cellular assays. Similarly, a loss of cellular activity is notable for the 3-fluoro-substituted ring B compound **22a** (not shown, BRAF IC_{50} of 0.01 μM, pERK IC_{50} of 21 μM, and SRB GI_{50} of 100 μM) compared to its nonmethylated counterpart **21d**.

Methylation at the N3 position is detrimental with a significant drop of potency in all three assays (**23a**, **23b**, and **23c**). The N3 of the imidazolone, facing the hinge backbone,[15] does not tolerate a substitution. These results suggest that the bulkier naphthyl ring B subtly shifts the position of the hinge-binding group A with respect to the published unsubstituted compounds and possibly that hydrogen bonding of NH-3 of the imidazolone with the hinge occurs to a certain extent for these compounds.

B−C Linker Modifications. To improve the bioavailability of these BRAF inhibitors, we synthesized compounds with one less NH-bond donor in the B−C linker (Table 4). Unfortunately, the replacement of the urea linker for a methylene amide or an amide leads to inactive compounds (cf **24a** vs **21t** and **25b** vs **22f**).

Linear Relationship between pERK IC_{50} and SRB GI_{50}. Linear regression analysis of the pERK IC_{50} and SRB GI_{50} values of 29 of the inhibitors synthesized shows a high correlation (eq 1), as the regression coefficient r is 0.87 (r^2 = 0.757) (see Figure 3). This analysis was performed using TSAR.[24]

$$\mathrm{SRB}(GI_{50}) = 2.41\mathrm{pERK}(IC_{50}) - 0.77$$
$$n = 29 \quad s = 3.80 \quad f = 81.21 \qquad (1)$$

These data indicate that there is a significant correlation between the SRB GI_{50} and the pERK IC_{50}. This finding provides evidence that the inhibition of growth of the mutant BRAF driven cells is an on-target effect.

Selectivity Studies. Our inhibitors were elaborated into the BPI pocket in an attempt to provide selectivity for mutant BRAF compared to other similar kinases. In this, we were successful for the three compounds (**21n**, **21u**, and **21x**) we submitted to the MRC National Centre for Protein Kinase Profiling and which were assessed at a single concentration of 1 μM. The three compounds are highly selective, hitting only a few kinases against the assessed panel of 69 (Figure 4). Src, Lck, and p38 (MAP) kinases are common hits with the three compounds, with **21u** showing selectivity toward the β isoform of p38 with respect to the α one.

Not surprisingly, the same three proteins have been shown to be sensitive to ligands that elaborate into the BPI pocket. This is the case of the recently released cocrystal structure of nilotinib[25] with p38β, and of the ones of imatinib with Src[26] and Lck.[27] In all those structures, the methylated central ring fits into the BPI pocket. Doramapimod, an inhibitor with similarity to some of our compounds, is a highly selective inhibitor of p38 MAP kinase[28,16] and presents a naphthyl moiety interacting with the BP1 pocket.

A cell selectivity experiment was also carried out. Growth inhibition for sorafenib and **22c** was performed against the WM266.4 (BRAF mutant) and WM1361 (NRAS mutant) cell lines (Figure 5). While no differential was observed in the case

Scheme 6. Formation of the B−C Urea Linker; Synthesis of Final Compounds via Route A

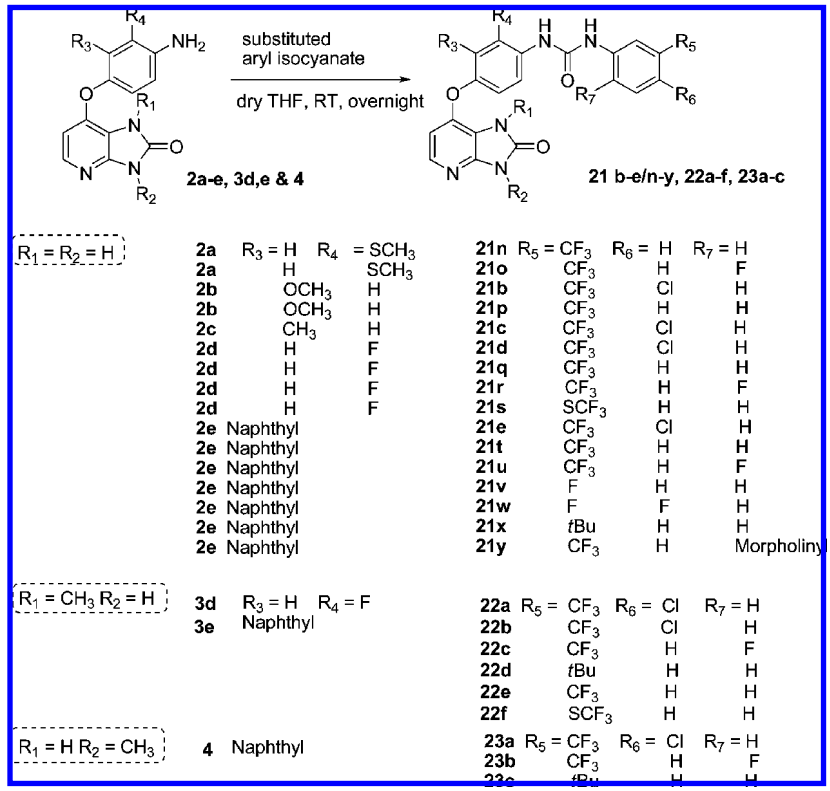

Scheme 7. Synthesis of Compounds with Amide and Methylene Amide Linker B−C via Route A

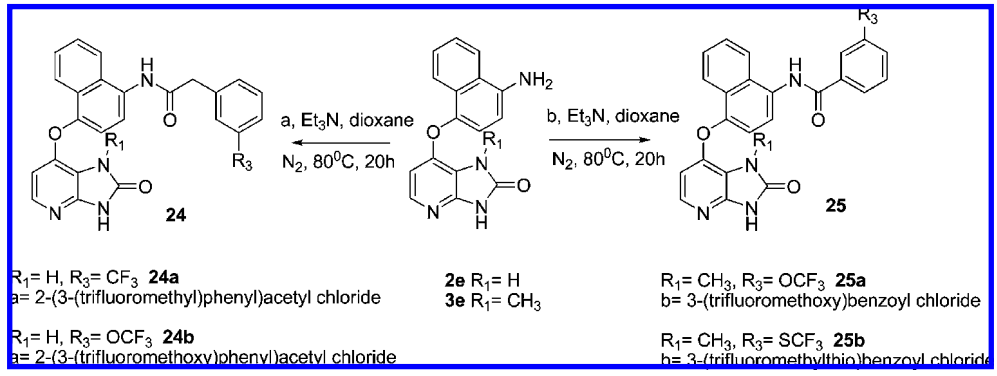

of sorafenib, a 6-fold difference is observed between the two cell lines for **22c**.

Conclusions

Following the development of a series of ^{V600E}BRAF inhibitors based on a novel hinge-binding fragment,[15] we have extended their scope by modifying the central phenyl ring. Our investigations show that ring B modification leads to a spectrum of low nanomolar inhibitors of ^{V600E}BRAF. In a number of examples, notably by ring B functionalization with fluoro, thiomethyl groups, or replacement with a naphthyl, highly potent inhibitors are obtained with IC_{50} values up to an order of magnitude lower than those for analogues with unsubstituted phenyl rings B. Seven compounds have an IC_{50} on ^{V600E}BRAF of less than 10 nM, and compounds **21a** and **21n**, each substituted with a thiomethyl group, notably achieve a ^{V600E}BRAF IC_{50} of 1 nM. Moreover, this 3-thiomethyl substitution, as for the naphthyl group, increases the potency on cells greatly with GI_{50}s in the nanomolar range. ^{V600E}BRAF inhibition in cells, measured with the pERK assay, is also submicromolar for some of the reported compounds and correlates with the cell growth inhibition; this strongly supports the mode of action of the compounds in this series. We have shown that these compounds inhibit both the ^{V600E}BRAF isolated enzyme and the enzyme in cellular assays and that this effect translates to potent inhibition of the growth of a mutant BRAF dependent melanoma cell line. Several of these compounds achieve over 10-fold increase in cellular potency compared to the reported BRAF inhibitor sorafenib. Furthemore, we have shown that elaborating the phenyl middle ring into the BPI pocket provides protein kinase and cell selectivities. These promising data warrant further in vivo investigation of this series.

Experimental Section

General Information. All starting materials, reagents, and solvents for reactions were reagent grade and used as purchased. Chromatography solvents were HPLC grade and were used without further purification. Reactions were monitored by thin-layer chromatography (TLC) analysis using Merck silica gel 60 F-254 thin layer plates. Flash column chromatography was carried out on

Scheme 8. Access to Final Compounds **21a**/**f**−**m** and **26** via Route B[a]

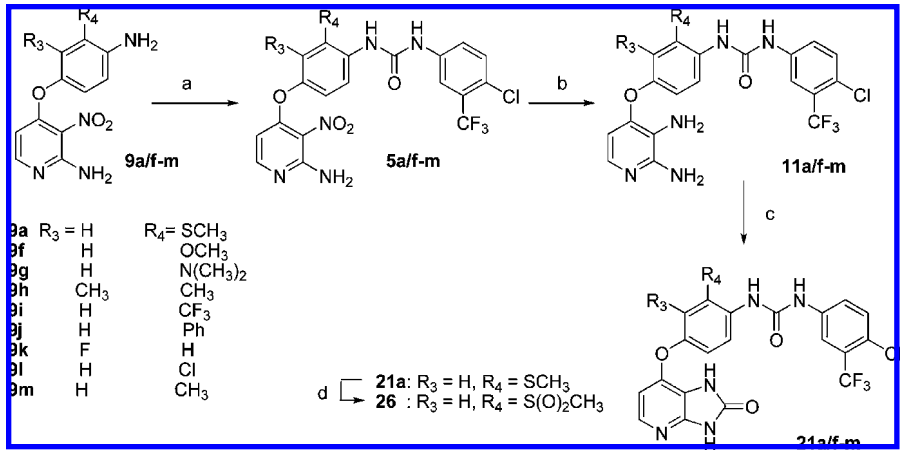

[a] Reagents and conditions: (a) 4-chloro-3-trifluoromethylphenylisocyanate in DCM or THF at room temperature, Ar atm; (b) Pd/C, H_2, RT or Fe, NH_4Cl in EtOH/H_2O, reflux for **9a**; (c)$(Cl_3CO)_2CO$, pyridine, THF, room temperature; (d) oxone, 0 °C.

Merck silica gel 60 (0.015−0.040 mm) or in disposable Isolute Flash Si and Si II silica gel columns. Preparative TLC was performed on either Macherey-Nagel [809 023] precoated TLC plates SIL G-25 UV_{254} or Analtech [2015] precoated preparative TLC plates, 2000 μm with UV_{254}. LC-MS analyses were performed on a Micromass LCT/Water's Alliance 2795 HPLC system with a Discovery 5 μm, C18, 50 mm × 4.6 mm i.d. column from Supelco at a temperature of 22 °C using the following solvent system: solvent A, methanol; solvent B, 0.1% formic acid in water, at a flow rate of 1 mL/min. Gradient starting with 10% A/90% B from 0 to 0.5 min then 10% A/90% B to 90% A/10% B from 0.5 to 6.5 min and continuing at 90% A/10% B up to 10 min. From 10 to 10.5 min, the gradient reverted back to 10% A/90% B and was held until 12 min. UV detection was at 254 nm, and ionization was positive or negative ion electrospray. The molecular weight scan range was 50−1000. Samples were supplied as 1 mg/mL in DMSO or methanol with 3 μL injected on a partial loop fill. NMR spectra were recorded on a Bruker DPX 250 MHz or a Bruker Advance 500 MHz spectrometer. The signal of the deuterated solvent was used as internal reference. Chemical shifts (δ) are given in ppm and are referenced to residual, not fully deuterated solvent signal (e.g., DMSO-d_5). Coupling constants (J) are given in Hz. The purity of the final compounds was determined by HPLC as described above and is 95% or higher unless specified otherwise.

Procedure A: 1-(4-(2,3-Dihydro-2-*oxo*-1*H*-imidazo[4,5-*b*]pyridin-7-yloxy)-2-(methylthio) phenyl)-3-(4-chloro-3-(trifluoromethyl)phenyl)urea (21a). 1-(4-(2,3-Diaminopyridin-4-yloxy)-2-(methylthio)phenyl)-3-(4-chloro-3-(trifluoromethyl)phenyl)urea **11a** (1.52 g, 3.1 mmol) was dissolved in dry THF (41 mL), and pyridine (2 mL) was added and the solution was cooled at 0 °C. Triphosgene (3.1 mmol) in dry THF (20 mL) was added dropwise. The reaction mixture was stirred for 15 min more at 0 °C and at room temperature for 16 h. The solvent was evaporated and the residue washed with water to provide after filtration the title compound (1.55 g, 97%) as a brown powder. ^{1}H NMR δ: 2.45 (s, 3H, CH_3), 6.42 (d, 1H, J smd 4.2, H_{Py}), 6.99 (d, 1H, J smd 8.4, H_{arom}), 7.19 (s, 1H, H_{arom}), 7.63 (s, 2H, H_{arom}), 7.78 (s, 2H, H_{arom}), 8.12 (s, 1H, H_{arom}), 8.26 (s, 1H, NH_{urea}), 9.91 (s, 1H, NH_{urea}), 11.25 (s, 1H, NH_{Py}), 11.44 (bs, 1H, NH_{Py}). ^{13}C NMR δ: 15.7, 105.7, 113.2, 116.4, 116.5, 117.3, 121.7, 122.2, 122.7, 123.8, 124.4, 131.9, 132.0, 133.1, 139.4, 141.1, 145.4, 146.8, 150.5, 152.6, 154.1. LC-MS: m/z 510 ([M + H]$^+$, 100). HRMS: m/z calcd for $C_{21}H_{15}ClF_3N_5O_3S$ ([M + H]$^+$): 510.0611; found: 510.0614.

Compounds **21f**−**m** were synthesized in a similar manner. The data are available in Supporting Information.

Procedure B: 1-(4-(2,3-Dihydro-2-*oxo*-1*H*-imidazo[4,5-*b*]pyridin-7-yloxy)-3-methoxyphenyl)-3-(4-chloro-3-(trifluoromethyl)phenyl)-urea (21b). 7-(4-Amino-2-methoxyphenoxy)-1*H*-imidazo[4,5-b]-pyridin-2(3*H*)-one **2b** (16 mg, 0.06 mmol) and corresponding substituted arylisocyanate (1.1 equiv) in anhydrous THF were stirred at room temperature for 14 h. The solvent was evaporated and the solid residue was washed with Et_2O to afford after filtration the title compound (28 mg, 98%) as a pale-yellow powder. ^{1}H NMR δ: 3.75 (s, 3H, CH_3), 6.05 (d, 1H, J = 5.8, H_{Py}), 7.05 (d, 1H, J = 8.7, H_{arom}), 7.26 (dd, 1H, J = 8.6 and J = 1.9, H_{arom}), 7.56 (d, 1H, J = 8.8, H_{arom}), 7.60 (d, 1H, J = 5.8, H_{Py}), 7.65 (d, 1H, J = 2.1, H_{arom}), 7.90 (m, 1H, H_{arom}), 8.28 (d, 1H, J = 2.4, H_{arom}), 10.02 (bs, 2H, NH_{urea}), 10.82 (bs, 1H, NH_{Py}), 10.98 (bs, 1H, NH_{Py}). ^{13}C NMR δ: 55.7, 104.3, 106.2, 111.0, 112.5, 116.8, 122.2, 122.4, 123.2, 124.0, 126.5, 131.7, 136.2, 138.8, 140.3, 151.2, 151.5, 153.1, 153.8, 156.2, 162.3. LC-MS: m/z 494 ([M + H]$^+$, 100). HRMS: m/z calcd for $C_{21}H_{15}ClF_3N_5O_4$ ([M + H]$^+$): 494.0837; found: 494.0836.

Compounds **21c**−**e**/**n**-**y**; **22a**−**f**; **23a**−**c** were synthesized in a similar manner. The data are available in Supporting Information.

Procedure C: *N*-(4-(2-*oxo*-2,3-dihydro-1*H*-imidazo[4,5-*b*]pyridin-7-yl-oxy)naphthalen-1-yl)-aminocarbonylmethylene-(3-trifluoromethyl-phenyl) (24a). To 7-(4-aminonaphthalen-1-yloxy)-1*H*-imidazo[4,5-*b*]pyridin-2(3*H*)-one **2e** (50 mg, 0.17 mmol) in anhydrous dioxane (7 mL), triethylamine (150 μL), and 2-(3-(trifluoromethyl)phenyl)acetyl chloride (0.20 mmol) were added under stirring and nitrogen atmosphere and heated for 20 h at 80 °C. The solvent was evaporated under vacuum and the solid residue dissolved in 10 mL of EtOAc and washed successively with brine (2 × 10 mL), a solution of citric acid, and brine again. The organic solution was evaporated under vacuum, and the solid residue recrystallized from EtOAc to afford the title compound (59 mg, 67%). ^{1}H NMR δ: 3.97 (s, 2H, CH_2), 6.24 (d, 1H, J = 5.9, H_{Py}), 7.26 (d, 1H, J = 8.2, H_{arom}), 7.58−7.74 (m, 7H, H_{arom} + H_{Py}), 7.81 (s, 1H, H_{arom}), 7.98 (d, 1H, J = 8.2, H_{arom}), 8.12 (d, 1H, J= 8.4, H_{arom}), 10.29 (s, 1H, NH_{amide}), 11.38 (s, 1H, NH_{Py}), 11.44 (s, 1H, NH_{Py}). LC-MS: m/z 479 ([M + H]$^+$, 100). HRMS: m/z calcd for $C_{25}H_{17}F_3N_4O_3$ ([M + H]$^+$) 479.1331; found 479.1318.

Compounds **24b**, **25a**,**b** were synthesized in a similar manner. The data are available in the Supporting Information.

1-(4-Chloro-3-(trifluoromethyl)phenyl)-3-(2-(methylsulfonyl)-4-(2-*oxo*-2,3-dihydro-1*H*-imidazo[4,5-*b*]pyridin-7-yloxy)phenyl)-urea (26). To a slurry of compound **21a** 1-(4-(2,3-dihydro-2-oxo-1*H*-imidazo[4,5-*b*]pyridin-7-yloxy)-2-(methylthio)phenyl)-3-(4-chloro-3-(trifluoromethyl)phenyl)urea (35 mg, 0.07 mmol) in MeOH (700 μL) was added slowly a solution of oxone (5 equiv) in water (900 μL). The mixture maintained at 0 °C was stirred 5 h and then neutralized with a saturated solution of $NaHCO_3$ to pH 8. The mixture was diluted in water and then filtered to provide the expected sulfone as a powder (22 mg, 60%). ^{1}H NMR δ: 3.32 (s, 3H, CH_3), 6.58 (d, 1H, J smd 5.8, H_{Py}), 7.51 (dd, 1H, J smd 8.9 and J smd 2.7, H_{arom}), 7.54 (d, 1H, J smd 2.7, H_{arom}), 7.64 (d, 1H, J smd 8.7, H_{arom}), 7.70 (d, 1H, J = 8.1, H_{arom}), 7.83 (d, 1H, J = 5.8, H_{Py}), 8.11 (m, 1H, H_{arom}), 8.14 (d, 1H, J = 8.9, H_{arom}), 8.64 (s,

1H, NH_{urea}), 10.29 (s, 1H, NH_{urea}), 11.21 (s, 1H, NH_{Py}), 11.45 (bs, 1H, NH_{Py}). ^{13}C NMR δ: 42.7, 106.7, 113.7, 116.9, 118.5, 121.6, 123.0, 123.8, 125.2, 126.3, 126.6, 130.2, 131.9, 133.3, 139.0, 141.3, 143.9, 147.2, 149.7, 151.9, 154.1. LC-MS: *m/z* 542 ($[M + H]^+$, 100). HRMS: *m/z* calcd for $C_{21}H_{15}ClF_3N_5O_5S$ ($[M + H]^+$): 542.0507; found: 542.0503.

Acknowledgment. This work is supported by Cancer Research UK (refs: C309/A2187 and C107/A10433), the Wellcome Trust, the Isle of Mann Anti-Cancer Association, and The Institute of Cancer Research. We acknowledge NHS funding to the NIHR Biomedical Research Centre. Professors Paul Workman and Julian Blagg are acknowledged for their strong support and helpful reading of the manuscript. Meirion Richards and Dr. Amin Mirza are thanked for providing technical assistance.

Supporting Information Available: Experimental protocols and analytical data for final compounds **21f**−**m**, **21c**−**e**/**n**−**y**, **22a**−**f**, **23a**−**c**, **24b**, **25a**,**b**, and all intermediates **2a**−**e**, **3d**,**e**, **4**, **5a/f**−**m**, **6a/f/g**, **7a**−**d/f**−**j**, **8a/d**, **9a**−**c/e**−**m**, **10a**−**e**, **11a/f**−**m**, **12a**−**e**, **13a**−**e**, **14d**,**e**, **15d**,**e**, **16d**,**e**, **18**, **19**, **20**, and protocols for biological assays. This material is available free of charge via the Internet at http://pubs.acs.org.

References

(1) Robinson, M. J.; Cobb, M. H. Mitogen-activated protein kinase pathways. *Curr. Opin. Cell Biol.* **1997**, *9*, 180–186.
(2) Cohen, P. Protein kinases—the major drug targets of the twenty-first century. *Nat. Rev. Drug Discovery* **2002**, *1*, 309–315.
(3) Davies, H.; Bignell, G. R.; Cox, C.; Stephens, P.; Edkins, S.; Clegg, S.; Teague, J.; Woffendin, H.; Garnett, M. J.; Bottomley, W.; Davis, N.; Dicks, N.; Ewing, R.; Floyd, Y.; Gray, K.; Hall, S.; Hawes, R.; Hughes, J.; Kosmidou, V.; Menzies, A.; Mould, C.; Parker, A.; Stevens, C.; Watt, S.; Hooper, S.; Wilson, R.; Jayatilake, H.; Gusterson, B. A.; Cooper, C.; Shipley, J.; Hargrave, D.; Pritchard-Jones, K.; Maitland, N.; Chenevix-Trench, G.; Riggins, G. J.; Bigner, D. D.; Palmieri, G.; Cossu, A.; Flanagan, A.; Nicholson, A.; Ho, J. W. C.; Leung, S. Y.; Yuen, S. T.; Weber, B. L.; Siegler, H. F.; Darrow, T. L.; Paterson, H.; Marais, R.; Marshall, C. J.; Wooster, R.; Stratton, M. R.; Futreal, P. A. Mutations of the BRAF gene in human cancer. *Nature* **2002**, *417*, 949–954.
(4) Wan, P. T. C.; Garnett, M. J.; Roe, S. M.; Lee, S.; Niculescu-Duvaz, D.; Good, V. M.; Jones, C. M.; Marshall, C. J.; Springer, C. J.; Barford, D.; Marais, R.; Cancer Genome, P. Mechanism of activation of the RAF-ERK signaling pathway by oncogenic mutations of B-RAF. *Cell* **2004**, *116*, 855–867.
(5) Karasarides, M.; Chiloeches, A.; Hayward, R.; Niculescu-Duvaz, D.; Scanlon, I.; Friedlos, F.; Ogilvie, L.; Hedley, D.; Martin, J.; Marshall, C. J.; Springer, C. J.; Marais, R. B-RAF is a therapeutic target in melanoma. *Oncogene* **2004**, *23*, 6292–6298.
(6) Friday, B. B.; Adjei, A. A. Advances in targeting the Ras/Raf/MEK/Erk mitogen-activated protein kinase cascade with MEK inhibitors for cancer therapy. *Clin. Cancer Res.* **2008**, *14*, 342–346.
(7) Brown, A. P.; Carlson, T. C. G.; Loi, C. M.; Graziano, M. J. Pharmacodynamic and toxicokinetic evaluation of the novel MEK inhibitor, PD0325901, in the rat following oral and intravenous administration. *Cancer Chemother. Pharmacol.* **2007**, *59*, 671–679.
(8) Davies, B. R.; Logie, A.; McKay, J. S.; Martin, P.; Steele, S.; Jenkins, R.; Cockerill, M.; Cartlidge, S.; Smith, P. D. AZD6244 (ARRY-142886), a potent inhibitor of mitogen-activated protein kinase/extracellular signal-regulated kinase kinase 1/2 kinases: mechanism of action in vivo, pharmacokinetic/pharmacodynamic relationship, and potential for combination in preclinical models. *Mol. Cancer Ther.* **2007**, *6*, 2209–2219.
(9) Sala, E.; Mologni, L.; Truffa, S.; Gaetano, C.; Bollag, G. E.; Gambacorti-Passerini, C. BRAF silencing by short hairpin RNA or chemical blockade by PLX4032 leads to different responses in melanoma and thyroid carcinoma cells. *Mol. Cancer Res.* **2008**, *6*, 751–759.
(10) Ramurthy, S.; Subramanian, S.; Aikawa, M.; Amiri, P.; Costales, A.; Dove, J.; Fong, S.; Jansen, J. M.; Levine, B.; Ma, S.; McBride, C. M.; Michaelian, J.; Pick, T.; Poon, D. J.; Girish, S.; Shafer, C. M.; Stuart, D.; Sung, L.; Renhowe, P. A. Design and Synthesis of Orally Bioavailable Benzimidazoles as Raf Kinase Inhibitors. *J. Med. Chem.* **2008**, *51*, 7049–7052.
(11) Sebolt-Leopold, J. S.; Herrera, R. Targeting the mitogen-activated protein kinase cascade to treat cancer. *Nat. Rev. Cancer* **2004**, *4*, 937–947.
(12) Adjei, A. A.; Cohen, R. B.; Franklin, W.; Morris, C.; Wilson, D.; Molina, J. R.; Hanson, L. J.; Gore, L.; Chow, L.; Leong, S.; Maloney, L.; Gordon, G.; Simmons, H.; Marlow, A.; Litwiler, K.; Brown, S.; Poch, G.; Kane, K.; Haney, J.; Eckhardt, S. G. Phase I pharmacokinetic and pharmacodynamic study of the oral, small-molecule mitogen-activated protein kinase kinase 1/2 inhibitor AZD6244 (ARRY-142886) in patients with advanced cancers. *J. Clin. Oncol.* **2008**, *26*, 2139–2146.
(13) Niculescu-Duvaz, I.; Roman, E.; Whittaker, S. R.; Friedlos, F.; Kirk, R.; Scanlon, I. J.; Davies, L. C.; Niculescu-Duvaz, D.; Marais, R.; Springer, C. J. Novel inhibitors of B-RAF based on a disubstituted pyrazine scaffold. Generation of a nanomolar lead. *J. Med. Chem.* **2006**, *49*, 407–416.
(14) Niculescu-Duvaz, I.; Roman, E.; Whittaker, S. R.; Friedlos, F.; Kirk, R.; Scanlon, I. J.; Davies, L. C.; Niculescu-Duvaz, D.; Marais, R.; Springer, C. J. Novel inhibitors of the v-raf murine sarcoma viral oncogene homologue B1 (BRAF) based on a 2,6-disubstituted pyrazine scaffold. *J. Med. Chem.* **2008**, *51*, 3261–3274.
(15) Niculescu-Duvaz, D.; Gaulon, C.; Dijkstra, H. P.; Niculescu-Duvaz, I.; Zambon, A.; Ménard, D.; Suijkerbuijk, B. M. J. M.; Nourry, A.; Davies, L.; Manne, H.; Friedlos, F.; Ogilvie, L.; Hedley, D.; Whittaker, S.; Kirk, R.; Gill, A.; Taylor, R. D.; Raynaud, F. I.; Moreno-Farre, J.; Marais, R.; Springer, C. J. Pyridoimidazolones as Novel Potent Inhibitors of v-Raf Murine Sarcoma Viral Oncogene Homologue B1 (BRAF). *J. Med. Chem.* **2009**, *52*, 2255–2264.
(16) Liao, J. J. L. Molecular recognition of protein kinase binding pockets for design of potent and selective kinase inhibitors. *J. Med. Chem.* **2007**, *50*, 409–424.
(17) Cervera, M.; Marquet, J.; Martin, X. Charge control in the SNAr reaction. Meta substitution with respect to the activating nitro group in 3,4-dihalogenonitrobenzenes. *Tetrahedron* **1996**, *52*, 2557–2564.
(18) Langer, O.; Dolle, F.; Valette, H.; Halldin, C.; Vaufrey, F.; Fuseau, C.; Coulon, C.; Ottaviani, M.; Nagren, K.; Bottlaender, M.; Maziere, B.; Crouzel, C. Synthesis of high-specific-radioactivity 4- and 6-[F-18]fluorometaraminol-PET tracers for the adrenergic nervous system of the heart. *Bioorg. Med. Chem.* **2001**, *9*, 677–694.
(19) Avenoza, A.; Busto, J. H.; Cativiela, C.; Peregrina, J. M. New efficient synthesis of 4-amino-3-arylphenols. *Synthesis Stuttgart* **1995**, 671–674.
(20) Winn, M.; Reilly, E. B.; Liu, G.; Huth, J. R.; Jae, H. S.; Freeman, J.; Pei, Z. H.; Xin, Z. L.; Lynch, J.; Kester, J.; von Geldern, T. W.; Leitza, S.; DeVries, P.; Dickinson, R.; Mussatto, D.; Okasinski, G. F. Discovery of novel *p*-arylthio cinnamides as antagonists of leukocyte function-associated antigen-1/intercellular adhesion molecule-1 interaction. 4. Structure−activity relationship of substituents on the benzene ring of the cinnamide. *J. Med. Chem.* **2001**, *44*, 4393–4403.
(21) Kundu, N. G.; Nandi, B. Palladium-copper catalyzed synthesis of benzofused heterocycles with two heteroatoms: Novel and highly regio- and stereoselective syntheses of (*E*)-2-(2-arylvinyl)-3-tosyl-2,3-dihydro-1,3-benzothiazoles and (*E*)-2-alkyl(aryl)idene-3,4-dihydro-2*H*-1,4-benzothiazines. *J. Org. Chem.* **2001**, *66*, 4563–4575.
(22) Chankeshwara, S. V.; Chakraborti, A. K. Indium(III) halides as new and highly efficient catalysts for *N*-*tert*-butoxycarbonylation of amines. *Synthesis* **2006**, 2784–2788.
(23) The phospho-ERK method is included in the Supporting Information.
(24) *TSARTM 3.3*; Oxford Molecular Limited: Oxford, UK, 2000.
(25) Filippakopoulos, P., Barr, A., Fedorov, O., Keates, T., Soundararajan, M., Elkins, J., Salah, E., Burgess-Brown, N., Ugochukwu, E., Pike, A. C. W., Muniz, J., Roos, A., Chaikuad, A., von Delft, F., Arrowsmith, C. H., Edwards, A. M., Weigelt, J., Bountra, C., Knapp, S. Crystal Structure of Human Mitogen Activated Protein Kinase 11 (p38 beta) in complex with Nilotinib. *Structural Genomics Consortium (SGC)* 2009; to be published.
(26) Seeliger, M. A.; Nagar, B.; Frank, F.; Cao, X.; Henderson, M. N.; Kuriyan, J. c-Src binds to the cancer drug imatinib with an inactive Abl/c-Kit conformation and a distributed thermodynamic penalty. *Structure* **2007**, *15*, 299–311.
(27) Jacobs, M. D.; Caron, P. R.; Hare, B. J. Classifying protein kinase structures guides use of ligand-selectivity profiles to predict inactive conformations: Structure of lck/imatinib complex. *Proteins: Struct., Funct., Bioinf.* **2008**, *70*, 1451–1460.
(28) Pargellis, C.; Tong, L.; Churchill, L.; Cirillo, P. F.; Gilmore, T.; Graham, A. G.; Grob, P. M.; Hickey, E. R.; Moss, N.; Pav, S.; Regan, J. Inhibition of p38 MAP kinase by utilizing a novel allosteric binding site. *Nat. Struct. Biol.* **2002**, *9*, 268–272.

JM900242C